Inorg. Chem. **2009**, *48*, 3679−3691

Studies on the Atropisomerism of Fe(II) 2,6-Bis(*N*-arylimino)pyridine Complexes†

Juan Cámpora,* M. Ángeles Cartes, Antonio Rodríguez-Delgado, A. Marcos Naz, Pilar Palma, and Carmen M. Pérez

Instituto de Investigaciones Químicas, CSIC, Universidad de Sevilla, c/ Américo Vespucio, 49, 41092, Sevilla, Spain

Diego del Rio

SRI International, 333 Ravenwsood Ave., Menlo Park, California 94065

Received November 26, 2008

NMR spectra of free 2,6-bis(*N*-arylimino)pyridine (PDI) ligands displaying different substituents at the ortho and ortho′ positions of the two *N*-aryl rings indicate that they can exist in syn (meso) and anti (chiral) configurations. These interconvert in solution at room temperature, via rotation of the aryl group. The corresponding paramagnetic FeX_2(PDI) complexes exhibit the same kind of isomerism, a property that is thought to be important for their activity as α-olefin polymerization catalysts. For the first time, this has been detected by ^{1}H NMR and studied in solution. Although the conformational stability of the diastereoisomeric complexes varies widely (depending on the size of the substituents at the imine and the aromatic rings), a moderate degree of steric hindrance suffices to allow their chemical separation. A simple procedure is developed for the preparation of these complexes in diastereoisomerically pure form. In addition, introduction of a prochiral substituent in the pyridine ring enables positive assignment of the stereoisomers. Isomerization rate measurements of the Fe(II) complexes in solution suggest that isomerization very likely involves the dissociation of the corresponding Fe−N(imino) bond prior to the rotation of *N*-aryl groups. DFT calculations provide additional support to the conformational assignment as well as the dissociative isomerization mechanism.

Introduction

Since the discovery of their catalytic properties nearly a decade ago,[1] iron and cobalt olefin complexes of 2,6-bis(imino)pyridine (PDI) ligands have become a paradigmatic group among homogeneous catalysts for polymerization or oligomerization. The high activity and the low toxicity of the iron catalysts[2] have contributed to the attraction of interest of both industry and academic research groups. A large number of FeX_2(PDI) catalysts have been prepared, covering different kinds of applications: not only polymerization of ethylene and propylene[1,3] but also α-olefin oligomerization[4] and polymerization of polar monomers.[5] The partially modular design of the PDI ligands allows the variation of their stereoelectronic properties by relatively simple synthetic means, and appropriate modifications enable the introduction of binding sites in the molecule for catalyst immobilization.[6]

Due to potential practical applications, recent work in our laboratory has focused on the synthesis and study of a number of iron PDI complexes,[7] and on the development of methods to vary the substitution pattern of the organic ligand.[7b,c] In the course of this work, we observed that the ^{1}H NMR spectra of FeX_2(PDI) displaying different substituents at the ortho and ortho′ positions of the *N*-aryl groups

† Dedicated to Prof. Ernesto Carmona on the occasion of his 60th birthday.

* To whom correspondence should be addressed. E-mail: campora@iiq.csic.es.

(1) (a) Small, B. L.; Brookhart, M.; Bennett, A. A. *J. Am. Chem. Soc.* **1998**, *120*, 4049. (b) Britovsek, G. J. P.; Gibson, V. C.; Kimberley, B. S.; Maddox, P. J.; McTavish, S. J.; Solan, G. A.; White, A. J. P.; Williams, D. J. *Chem. Commun.* **1998**, 849. (c) Small, B. L.; Brookhart, M. *J. Am. Chem. Soc.* **1998**, *120*, 7143. (d) Gibson, V. C.; Spitzmesser, S. K. *Chem. Rev.* **2003**, *103*, 283.

(2) (a) *Chem. Eng. News* **2008**, *July 28*, 53. (b) Bart, S. C.; Lobkovsky, E.; Chirik, P. J. *J. Am. Chem. Soc.* **2004**, *126*, 13794. (c) Correa, A.; García-Mancheño, O.; Carsten Bolm, C. *Chem. Soc. Rev.* **2008**, *37*, 1108.

10.1021/ic802271y CCC: $40.75
Published on Web 03/16/2009

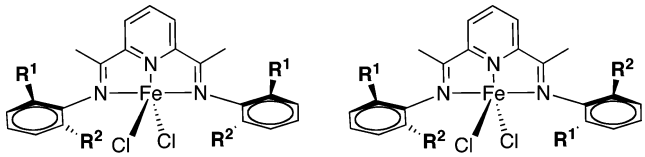

Figure 1. Atropisomerism in FeX_2(PDI).

indicate that they exist as a mixture of geometric isomers. This phenomenon is due to the restricted rotation of the *N*-aryl groups, which can adopt one of two possible dispositions, syn or anti, that is, a case of atropisomerism (Figure 1). While the syn configuration gives rise to a meso diastereoisomer (C_s symmetry), the anti results in a racemic mixture of enantiomeric isomers with C_2 symmetry. This traces an interesting parallelism with the well-known Zr *ansa*-metallocene complexes pioneered by Ewen and Brintzinger et al. as catalysts for stereoselective α-olefin polymerization.[8−10] Recently, we have shown that this analogy can be successfully extended to the domain of catalysis.[11] Although the stereoselectivity of FeX_2(PDI) complexes as propylene polymerization catalysts is dominated by a chain-end control mechanism, the isotacticity of polypropylene produced by a complex displaying the chiral anti configuration is significantly improved as compared to that obtained with the syn isomer. This points to the existence of a concurrent enantiomorphic site stereoregulation mechanism.

A number of authors preceded us by proposing that atropisomerism of FeX_2(PDI) complexes has important effects on their catalytic perfomance,[3a,k,12] but without providing direct evidence of its existence. Not only PDI-based catalysts but related systems, such as group 10 α-diimine complexes, might also be influenced by analogous sterochemical phenomena.[13] A number of X-ray diffraction structures of FeX_2(PDI) complexes with unsymmetrically substituted aryl rings have been reported. These often display a single diastereoisomer, either the syn[14] or the chiral anti.[15] Sometimes, both forms coexist in a single crystalline phase,[16] suggesting that these may also exist together in solution. Therefore, it is somewhat surprising that, in spite of their potential applications in stereoselective catalysis, there is virtually no information on the stereochemical stability of such isomers in solution. This might be due to the fact that, although these paramagnetic complexes give rise to useful ^{1}H NMR spectra, these may be difficult to interpret, and therefore they are not systematically recorded. In this article, we show that conformational isomerism of iron PDI complexes is readily detected in their solution NMR spectra. The stereochemical stability of these compounds varies widely, ranging from fast exchange on the NMR time scale to chemically separable isomers depending on the size of the substituents. This enables the study of the isomer exchange rates, which point to a dissociative mechanism for the mutual interconversion process.

Results and Discussion

Synthesis of Ligands and Complexes. Ligands and complexes employed in this work are shown in Chart 1. Most of the ligands were prepared by standard procedures, involving the condensation of 2,6-diacylpyridines or 2,6-diformylpyridines with the corresponding anilines under azeotropic water-removal conditions. Ligand **L9** was prepared from **L3** using a selective alkylation procedure recently reported by us.[7b]

Iron complexes were prepared by reacting the corresponding ligand with a suitable metal precursor ($FeCl_2 \cdot 4H_2O$, $FeCl_2$(dme), or anhydrous $FeBr_2$; dme = dimethoxyethane),

(3) See, for example: (a) Small, B. L.; Brookhart, M. *Macromolecules* **1999**, *32*, 2120. (b) Britovsek, G. J. P.; Bruce, M.; Gibson, V. C.; Kimberley, B. S.; Maddox, P. J.; Mastroianni, S.; McTavish, S. J.; Redshaw, C.; Solan, G. A.; Strömberg, S.; White, A. J. P.; Williams, D. J. *J. Am. Chem. Soc.* **1999**, *121*, 8728. (c) Britovsek, G. J. P.; Baugh, S. P. D.; Hoarau, O.; Gibson, V. C.; Wass, D. F.; White, A. J. P.; Williams, D. J. *Inorg. Chim. Acta* **2003**, *345*, 279. (d) Armspach, D.; Matt, D.; Peruch, F.; Lutz, P. *Eur. J. Inorg. Chem.* **2003**, *5*, 805. (e) Chen, J.; Huang, Y.; Li, Z.; Zhang, Z.; Wei, C.; Lan, T.; Zhang, W. *J. Mol. Catal. A: Chem.* **2006**, *259*, 133. (f) Amort, C.; Malaun, M.; Krajete, A.; Kopacka, H.; Wurst, K.; Christ, M.; Lilge, D.; Kristen, Marc, O.; Bildstein, B. *Appl. Organomet. Chem.* **2002**, *16*, 506. (g) Kaul, F. A. R.; Puchta, G. T.; Frey, G. D.; Herdtweck, E.; Herrmann, W. A. *Organometallics* **2007**, *26*, 988. (h) Boca, M.; Boca, R.; Kikelbick, G.; Linert, W.; Svoboda, I.; Fuess, H. *Inorg. Chim. Acta* **2002**, *36*, 338. (i) Smit, T. M.; Tomov, A. K.; Gibson, V. C.; White, A. J. P.; Williams, D. J. *Inorg. Chem.* **2004**, *43*, 6511. (j) Chen, Y.; Chen, R.; Qian, C.; Dong, X.; Sun, J. *Organometallics* **2003**, *22*, 4312. (k) Ionkin, A. S.; Marshall, W. J.; Adelman, D. J.; Fones, B. B.; Fish, B. M.; Schiffhauer, M. F. *Organometallics* **2006**, *25*, 2978.

(4) (a) Small, B. L.; Brookhart, M. *J. Am. Chem. Soc.* **1998**, *120*, 7143. (b) Britovsek, G. J. P.; Mastroianni, S.; Solan, G. A.; Baugh, S. P. D.; Redshaw, C.; Gibson, V. C.; White, A. J. P.; Williams, D. J.; Elsegood, M. R. J. *Chem.—Eur. J.* **2000**, *6*, 2221. (c) Small, A, B. L.; Marcucci, J. *Organometallics* **2001**, *20*, 5738. (d) Chen, Y.; Qian, C.; Sun, J. *Organometallics* **2003**, *22*, 1231. (e) Bianchini, C.; Giambastiani, G.; Rios Guerrero, I.; Meli, A.; Passaglia, E.; Gragnoli, T. *Organometallics* **2004**, *23*, 6087. (f) Tellmann, K. P.; Gibson, V. C.; White, A. J. P.; Williams, D. J. *Organometallics* **2005**, *24*, 280.

(5) Castro, P. M.; Lappalainen, K.; Ahlgrén, M.; Leskelä, M.; Repo, T. *J. Polym. Sci., Part A: Polym. Chem.* **2003**, *41*, 1380.

(6) (a) Kaul, F. A. R.; Puchta, G. T.; Schneider, H.; Bielert, F.; Mihalios, D.; Herrmann, W. A. *Organometallics* **2002**, *21*, 74. (b) Kim, I.; Han, B. H.; Ha, C.-S.; Kim, J.-K.; Suh, H. *Macromolecules* **2003**, *36*, 6689. (c) Jin., G.-X.; Zhang, D. J. *Polym. Sci. Polym. Chem.* **2004**, *42*, 1018.

(7) (a) Cámpora, J.; Naz, A. M.; Palma, P.; Álvarez, E.; Reyes, M. L. *Organometallics* **2005**, *24*, 4878. (b) Cámpora, J.; Pérez, C. M.; Rodríguez-Delgado, A.; Naz, A. M.; Palma, P.; Álvarez, E. *Organometallics* **2007**, *26*, 2104. (c) Cámpora, J.; Naz, A. M.; Rodríguez-Delgado, A.; Álvarez, E.; Tritto, I.; Boggioni, L. *Eur. J. Inorg. Chem.* **2008**, 1871.

(8) Razavi, A.; Thewalt, U. *J. Organomet. Chem.* **1993**, *445*, 111.

(9) (a) Ewen, J. A. *J. Am. Chem. Soc.* **1984**, *106*, 6355. (b) Ewen, J. A. In *Catalytic Polymerisation of Olefins, Studies in Surface Science and Catalysis*; Keii, T., Soga, K., Eds.; Elsevier: New York, 1986; p 271.

(10) (a) Kaminsky, W.; Kulper, K.; Brintzinger, H.-H.; Wild, F. R. W. P. *Angew. Chem., Int. Ed. Engl.* **1985**, *24*, 507. (b) Röll, W.; Brintzinger, H.-H.; Rieger, B.; Zolk, R. *Angew. Chem., Int. Ed. Engl.* **1990**, *29*, 279.

(11) Rodríguez-Delgado, A.; Cámpora, J.; Naz, A. M.; Palma, P.; Reyes, M. L. *Chem. Commun.* **2008**, 5230.

(12) Pellechia, C.; Pappalardo, D.; Mazzeo, M. *Macromol. Rapid Commun.* **1998**, *19*, 651.

(13) (a) Gates, D. P.; Svejda, S. A.; Oñate, E.; Killian, C. M.; Johnson, L. K.; White, P. S.; Brookhart, M. *Macromolecules* **2000**, *33*, 2320. (b) Pappalardo, D.; Mazzeo, M.; Antinucci, S.; Pellechia, C. *Macromolecules* **2000**, *33*, 9483. (c) Zou, H.; Ming Zhu, F.; Wu, Q.; Yan al, J.; An Lin, S. *J. Polym. Sci., Part A: Polym. Chem.* **2005**, *43*, 1325.

(14) Crystal structures of FePDI complexes displaying syn configuration (Cambridge Structural Database codes): FEQLUJ, FEQMAQ[4f]; MAZWEP, MAZWIT, MAZWOZ[4b]; and XALLEB[3a].

(15) Crystal structures of FePDI complexes displaying anti configuration (CSD codes): EKINAN[4d], QELJAT, QELJEX, and QELJIB[3k].

(16) Disordered FePDI structures (CSD codes): EMEHOT[3a]; QELJUN[3k].

Chart 1

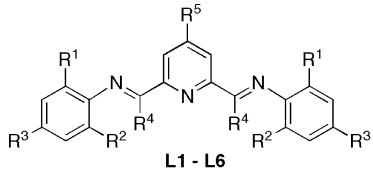

L1 - L6

	R^1	R^2	R^3	R^4	R^5
1	Me	Cl	Me	Me	H
2	*i*-Pr	Me	H	H	H
3	*i*-Pr	Me	H	Me	H
4	*i*-Pr	Me	H	*n*-Bu	H
5	*t*-Bu	H	H	Me	H
6	*t*-Bu	Me	*t*-Bu	Me	H
9	*i*-Pr	Me	H	Me	CH_2CMe_2Ph

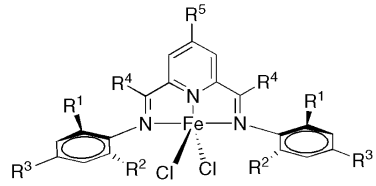

C1 - C6; C9

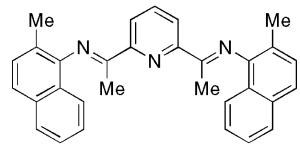

L7

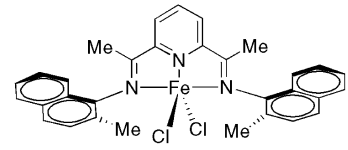

C7

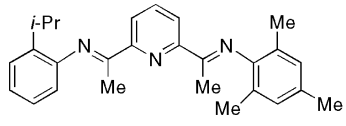

L8

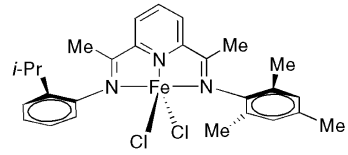

C8

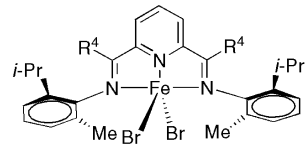

C3'

Scheme 1

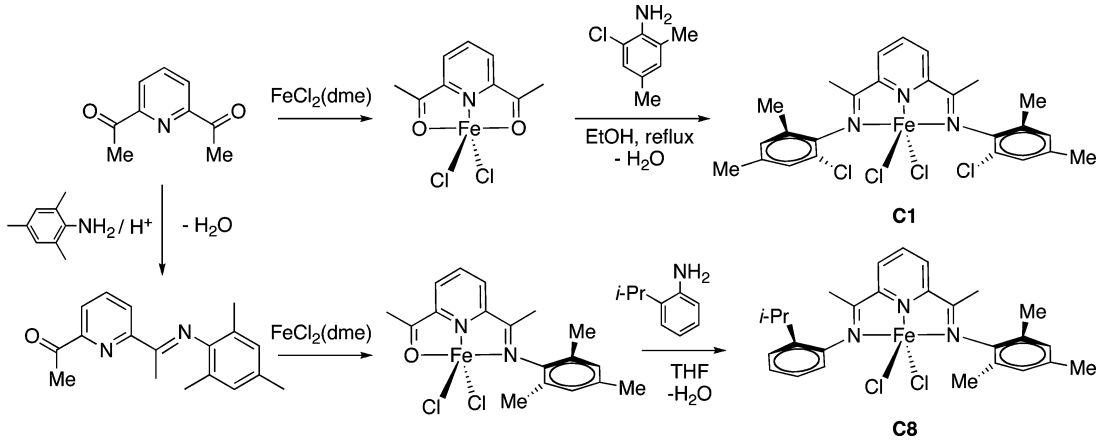

usually in THF. By selecting an appropriate combination of solvent and precursor, the products precipitated directly from the reaction mixture. All of them are dark-blue paramagnetic complexes, with effective magnetic moments in the range of 5.0−5.8 μ_B in the solid state (magnetic susceptibility balance), similar to the values reported by other authors.[3−5,12−16]

The methodology used for ligand synthesis did not provide satisfactory yields for **L1**, probably due to the low nucleophilicity of 2-chloro-4,6-dimethylaniline. In order to circumvent this problem, we avoided using this ligand in the synthesis of its Fe complex, **C1**. The alternative procedure (Scheme 1, top) involved the reaction of the above-mentioned aniline with the complex [$FeCl_2$(2,6-diacetylpyridine)]. The latter was obtained as a magenta paramagnetic solid when a suspension of $FeCl_2$(dme) was treated with 2,6-diacetylpyridine. The condensation reaction took place in refluxing

Chart 2

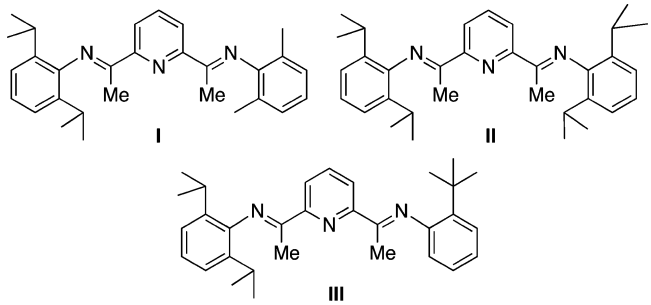

ethanol, cleanly affording **C1** in high yield. As shown in Scheme 1 (bottom), a similar approach also proved convenient for the synthesis of complexes displaying two different *N*-aryl groups, like **C8**. Many complexes of this kind have been reported in the literature, but the synthesis of the corresponding ligands by consecutive condensation reactions is often unselective and their isolation in pure form can be difficult. Thus, we prepared **L8** by the condensation of 2,6-diacetylpyridine with 1 equiv of 2,4,6-trimethylaniline to afford the corresponding monoimine, which was subsequently reacted with 2,6-diisopropyl aniline. While the selectivity of the first step could be controlled by using an excess of the diketone, the second one afforded a mixture of the desired ligand and the two symmetric diimines. The alternative route to complex **C8** involved, first, the preparation of the corresponding Fe complex of the monoimine. Similar *N*,*N*,*O* chelated complexes have been recently reported by Herrmann et al.[3g] The reaction of this complex with 2-isopropropylaniline under mild conditions selectively afforded the desired product.

Restricted Aryl Rotation in Free PDI Ligands. Before examining the isomerism of Fe−PDI complexes, it is important first to consider the ligands themselves. Although they are not affected by any of the complications associated with paramagnetic compounds, to the best of our knowledge, there are no literature references regarding their atropisomerism. Brookhart and Small observed that the rotation of the aryl groups is hindered by bulky substituents in the ortho positions.[3a] They mentioned that in the ^{1}H and ^{13}C NMR spectra of derivatives **I** and **II** (Chart 2) the Me's of the *i*Pr groups have diastereotopic character, each of them giving rise to one distinct signal. This indicates that the rotation of the 2,6-diisopropylphenyl groups is slow on the NMR time scale. The same was observed for the unsymmetrically substituted ligand **III**, albeit the presence of only one set of *i*Pr signals indicates that the 2-*t*-butylphenyl moiety rotates freely. These observations exemplify how isopropyl groups can be used to probe the rotation of aryl groups, even when the molecule is not susceptible to rotational isomerism.

Although the ^{1}H NMR spectrum of **L3** in $CDCl_3$ contains only one set of signals, it displays two distinct doublets for the isopropyl methyls, which indicate that the rotation of *o*-isopropyl-*o*′-methylphenyl rings is slow at room temperature. According to Brookhart and Small, this observation suggests that the compound exists as a single isomer in solution. However, we found that, on changing the solvent to C_6D_6, the *o*-methyl singlet and the two isopropyl methyl doublets split each of them in a pair of equally intense signals, revealing that this compound exists as a 1:1 mixture of isomers in solution. The magnitude of the splitting is very small (just a few hertz), and it is likely that in some solvents like $CDCl_3$ it simply cannot be resolved. The fact that this splitting only becomes noticeable for signals belonging to the ortho substituents clearly points to the rotation of the aryl groups as the source of isomerism. The ^{1}H NMR spectrum of **L6** in C_6D_6 or toluene-d_8 displays similar splitting of the ortho Me and *t*-Bu signals. In this case, we noticed that one of the two isomers prevails in freshly prepared samples, but the intensity ratio of each pair of signals gradually evolves until the 1:1 equilibrium ratio is attained. Measurements of the isomerization rate at different temperatures between 288 and 343 K give a free activation energy $\Delta G^{\ddagger}$ of 20.2(2) kcal mol^{-1} at 298 K. In contrast, the spectra of **L3** always display the same 1:1 equilibrium ratio, preventing direct measurement of the isomerization rate. However, its spectrum shows some line broadening above room temperature, as a consequence of the rapid rotation of the *N*-aryl groups. As can be seen in Figure 2, individual signals of the isomers coalesce into a single set of signals at 378 K. Above this temperature, the *i*Pr methyl signals continue to broaden and merge into a single broad resonance. The fast exchange limit, at which the diastereotopic character of the isopropyl methyl groups would be fully lost, could not be reached, but at the highest temperature studied (443

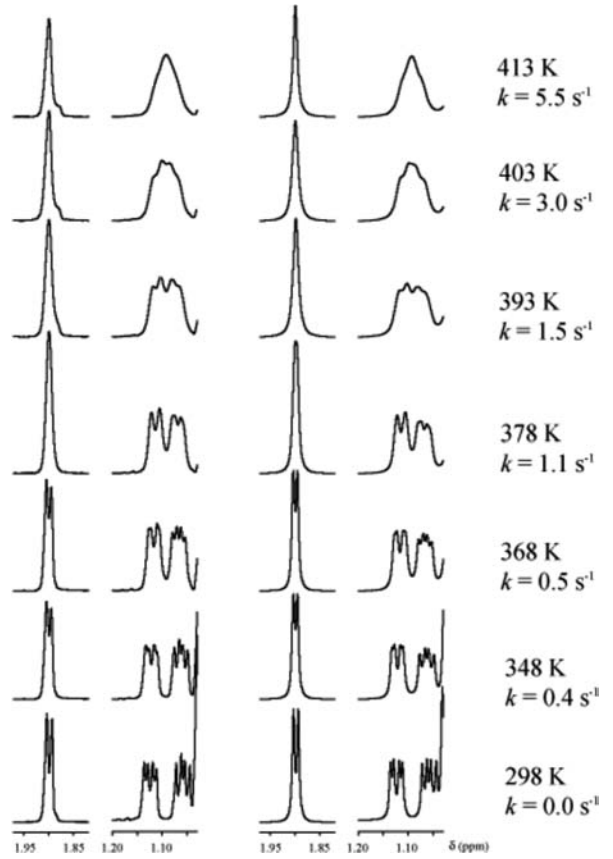

Figure 2. Experimental (left) and simulated (right) methyl region of the ^{1}H NMR signals (δ 1.90 ppm, *o*-Me; 1.05−1.15 ppm, *i*Pr) of **L3** at different temperatures. Temperatures and exchange rate constants are shown at the right-most part of the figure.

Table 1. Activation Parameters for Isomerization Processes

compound	R^1	R^2	R^4	X	T range (K)	equil. ratio	$\Delta H^{\ddagger}$ kcal/mol	$\Delta S^{\ddagger}$ cal/mol K	$\Delta G^{\ddagger}_{(298K)}$ kcal/mol
C3	Me	^{i}Pr	Me	Cl	296−326	1:1	25.5(8)	+5(3)	24.0(1)
C4	Me	^{i}Pr	^{n}Bu	Cl	296−326	1:1	25(3)	+5(10)	23.7(2)
C6	Me	^{t}Bu	Me	Cl	263−306	2:8	24(2)	+5(6)	22.3(2)
L3[a]	Me	iPr	Me		298−413	1:1	14(2)	−21(4)	20.7(1)
L6	Me	^{t}Bu	Me		288−319	1:1	16(2)	−13(7)	20.2(2)

[a] From NMR spectral simulation data.

K), there are clear signs of such coalescence. Also shown in Figure 2 is a full line shape simulation of the spectra, which provides the isomer exchange rates at each temperature. The activation parameters deduced from these data (see below, Table 1) are remarkably similar to those calculated for **L6**, in spite of the different techniques employed in the measurements. Thus, the value of the activation barrier, $\Delta G^{\ddagger}_{298}$, is the same for the two compounds within the experimental error.

Atropisomerism of Fe−PDI Complexes. The ^{1}H NMR spectra of the paramagnetic FeX_2(PDI) complexes **C1**−**C9** have been fully assigned on the basis of signal intensities and bandwidth. In spite of their wide breadth, and the rather unpredictable signal positions, they bear reasonable analogy, which facilitates the assignment task. Chemical shifts display the expected Curie dependency on T^{-1} and are reported at 20 °C unless otherwise stated. The resonances of the PDI pyridine and imine fragments display large isotropic shifts, due to the efficient spin delocalization along the ligand π orbitals. Thus, signals corresponding to the pyridine H3 and H4 atoms are invariably found in the low-field extreme of the spectrum (30−90 ppm), while the acetaldimine methyl resonates in the high-field side (−20 to −35 ppm). Since the orthogonal disposition of the ligand plane and the *N*-aryl groups hamper spin delocalization, the corresponding signals tend to appear closer to the diamagnetic region.

NMR spectra of complexes having two different ortho aryl substituents usually display two complete sets of signals, indicating that they exist as isomeric mixtures. In contrast with the free ligands, the large isotropic shifts characteristic of paramagnetic complexes facilitate the observation of the splitting of most of their signals. However, the separation of each signal pair is not large, in general less than a few parts per million, which prevents the observation of stereochemically significant trends. Isomeric splitting is never seen in complexes having one or two symmetrically substituted aryl groups. For example, the spectrum of the "mixed" complex **C8**, with a symmetric mesityl group, shows a single set of signals. The overall number of methyl signals (seven, including the two α-imino groups) can only be accounted for if the rotation of both aryl groups is slow on the NMR time scale. This rules out the square-pyramidal configuration of the iron center as the source of the observed isomerism, since this would lead to two possible isomers, as shown in Figure 3.[17]

As expected for atropisomerism, steric effects control the conformational stability of the isomers. As shown in Chart 3, three qualitative situations can be distinguished. The first is exemplified by complexes **C3**, **C3′**, **C4**, and **C6**, possessing relatively bulky substituents of the size of or larger than methyl at both aryl ortho positions and at the imine α carbon. Their interconversion is slow in solution at room temperature, and they can be fully or partially separated, as discussed below. The second group is formed by complexes having one ortho substituent smaller than a methyl group but larger than a hydrogen atom, for example, Cl (**C1**) or a fused benzo ring (**C7**). The ^{1}H-NMR spectra of these complexes display two distinct sets of signals, but the isomer exchange rate is too fast to allow their chemical separation. As the equilibrium situation is rapidly attained in solution, the NMR signals of the isomers always show the same intensity ratio, generally 1:1. Complexes that exhibit free rotation of the aryl groups at room temperature compose the third group. This is the case for **C2** and **C5**, with a hydrogen atom at either the imine α-carbon or at one of the aryl ortho positions. In these relatively unhindered molecules, free rotation of the *N*-aryl groups is responsible for the rapid exchange between the syn and anti configurations at room temperature. This is shown by the apparent loss of the diastereotopic character of the isopropyl methyl groups in **C2**, whose spectrum displays a single methyl resonance for 12 H at δ 1.12 ppm. The room-temperature ^{1}H NMR spectrum of **C5** provides no indication of whether the compound exists as two rapidly exchanging isomers or as a single, highly favored configuration. Seeking to clarify this point, we recorded the spectrum of **C5** at lower temperatures. A second set of signals with ca. 10% of the intensity of those of the major isomer can be observed below 263 K, the slow exchange limit being reached at 223 K. Although the paramagnetic line broadening and the low concentration of the minor isomer complicate the use of spectral line shape simulation to deduce the exchange rate constants, an estimation provides $\Delta G^{\ddagger}$ values of ca. 13 kcal mol^{-1} between 298 and 263 K. The size of this barrier indicates that the imine α-methyl still poses some hindrance to the rotation of the aryl group, even when one of the ortho positions remains unsubstituted. Note the difference with **C2**: in this case, apparent equivalent isopro-

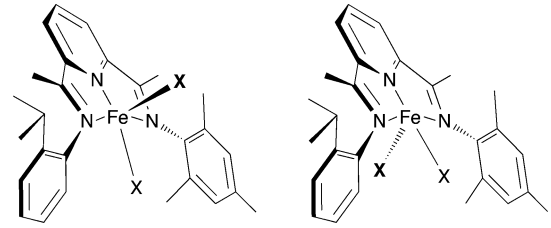

Figure 3. Isomerism due to the configuration of the metal center (not observed).

(17) The iron center is expected to invert its configuration very rapidly at room temperature. An energy barrier of ca. 10 kcal mol^{-1} has been measured for the organometallic complex $Fe(CH_2SiMe_3)_2$(PDI^{mes}) (PDI^{mes} = 2,6-bis(*N*-mesitylacetaldimino)pyridine (see ref 7a).

Chart 3

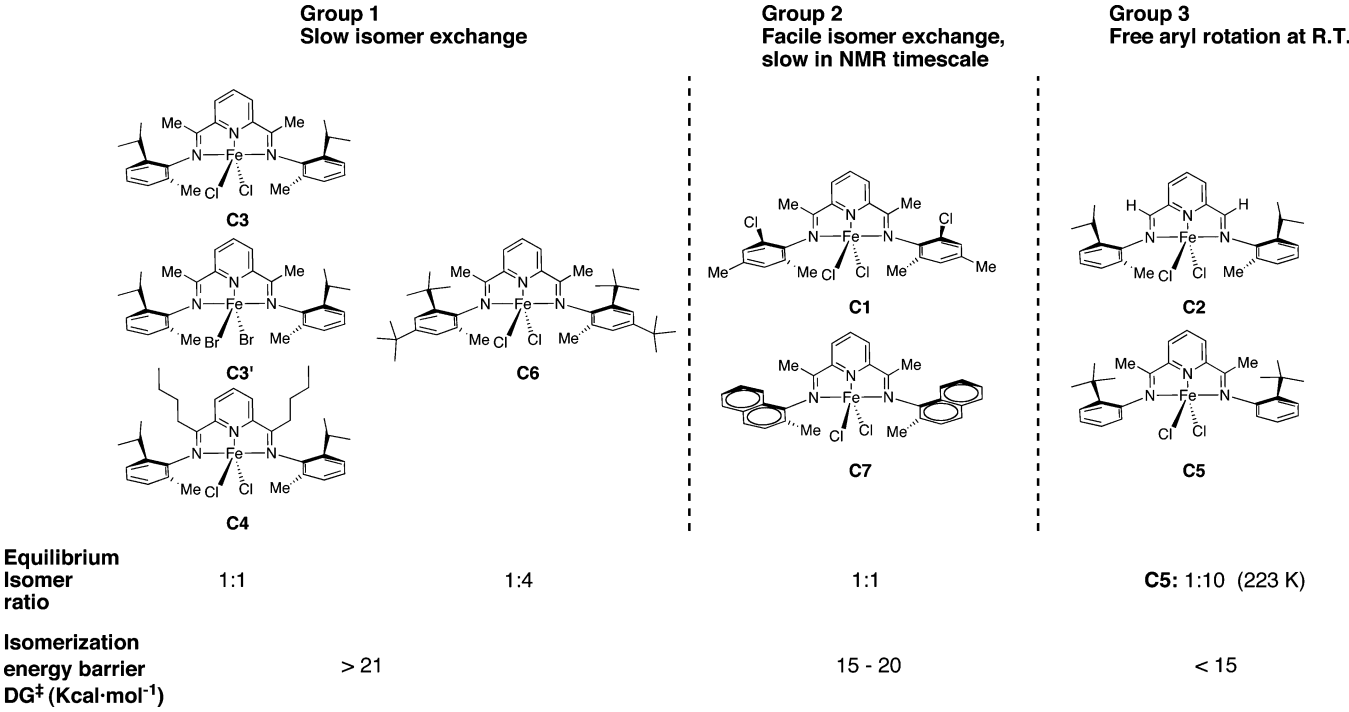

pyl methyl signals implies essentially unrestricted rotation of the aryl groups.[18]

Complexes with the highest degree of steric hindrance, such as **C3**, show interesting solubility behavior. ^{1}H NMR spectra of fresh samples of this product in CD_2Cl_2, prepared with the solid that precipitated from the reaction mixtures (THF), display one species as the prevalent (>90%) or even the only component. However, when these samples are left at room temperature over several hours or are gently warmed (40 °C), less intense signals grow at the expense of the other until a 1:1 ratio is attained. This is illustrated in Figure 4 (spectra A and B). Rapid evaporation of these samples to dryness does not restore the initial situation, but affords solid mixtures which retain the solution isomer ratio. Analytical and magnetic data gathered for these solid mixtures are identical to those of the original sample, confirming that the two species are indeed isomers. These observations indicate that, during its synthesis, **C3** selectively precipitates essentially as a single isomer, which becomes trapped in the solid state. Since in solution this isomer slowly equilibrates with the second one, and both are equally stable, the insolubility of the product in the reaction solvent (THF) is essential in order to generate isomerically pure samples.

Complexes **C3′** and **C4** behave similarly and they can be prepared as solid samples containing >90% of a single isomer, using $FeBr_2$ or hydrated iron chloride as precursors in THF. Equilibration of these compounds in CD_2Cl_2 at room temperature also affords 1:1 isomer mixtures. In the case of the more soluble complex **C6**, it is necessary to replace THF with diethyl ether and to use the more reactive reagent $FeCl_2$(dme), instead of simple iron salts. The NMR spectrum in CD_2Cl_2 of the precipitate displays two isomers in a 2.3:1 ratio. When this solution is left at room temperature, the isomer ratio gradually changes, eventually inverting its value to a 1:4 equilibrium composition. This indicates a slight but noticeable thermodynamic preference (ca. 0.8 kcal mol^{-1}) for one of the isomers, in contrast with the essentially degenerate equilibria observed in the preceding complexes.

In spite of our efforts, we have been unable to grow quality crystals of the former complexes for X-ray diffraction studies. However, NMR spectra of microcrystalline samples obtained by the slow evaporation of **C3** solutions in CH_2Cl_2 indicated the presence of a single species (**C3*s***). Interestingly, this is *not* the same isomer that precipitates during the synthesis (**C3*a***), but the second one observed after solution isomerization (see Figure 4). This behavior indicates that **C3*s*** is less soluble in CH_2Cl_2 and crystallizes selectively while the slow exchange process maintains the equilibrium in solution. Since the two isomers are equally stable in solution, but one is appreciably less soluble than the other, when a solid **C3*a*** and **C3*s*** mixture is stirred in a hexane/dichloromethane suspension (where they are only sparingly soluble), a continuous dissolution−crystallization process gradually shifts the isomer ratio in the solid phase until it is turned into essentially pure **C3*s*** (spectrum C, Figure 4). Reasoning that the cause of the selective formation of **C3*a*** during synthesis could also be a solubility effect, we stirred a suspension of **C3*a*** and **C3*s*** in THF for 24 h, and the initial composition of the solid (i.e., > 90% **C3*a***) was restored. These properties provide a simple and very convenient method to pertub isomeric mixtures of this compound, shifting their composition toward one or the other isomer

(18) The separation of the two diastereotopic isopropyl Me signals is usually very large in these paragmagnetic complexes, for example, 10.5 ppm in **C8**. Coalescence of such signals involves very high exchange rates (ca. 5×10^4 s^{-1} in a 400 MHz spectrometer), i. e., an energy barrier below 10 kcal mol^{-1}.

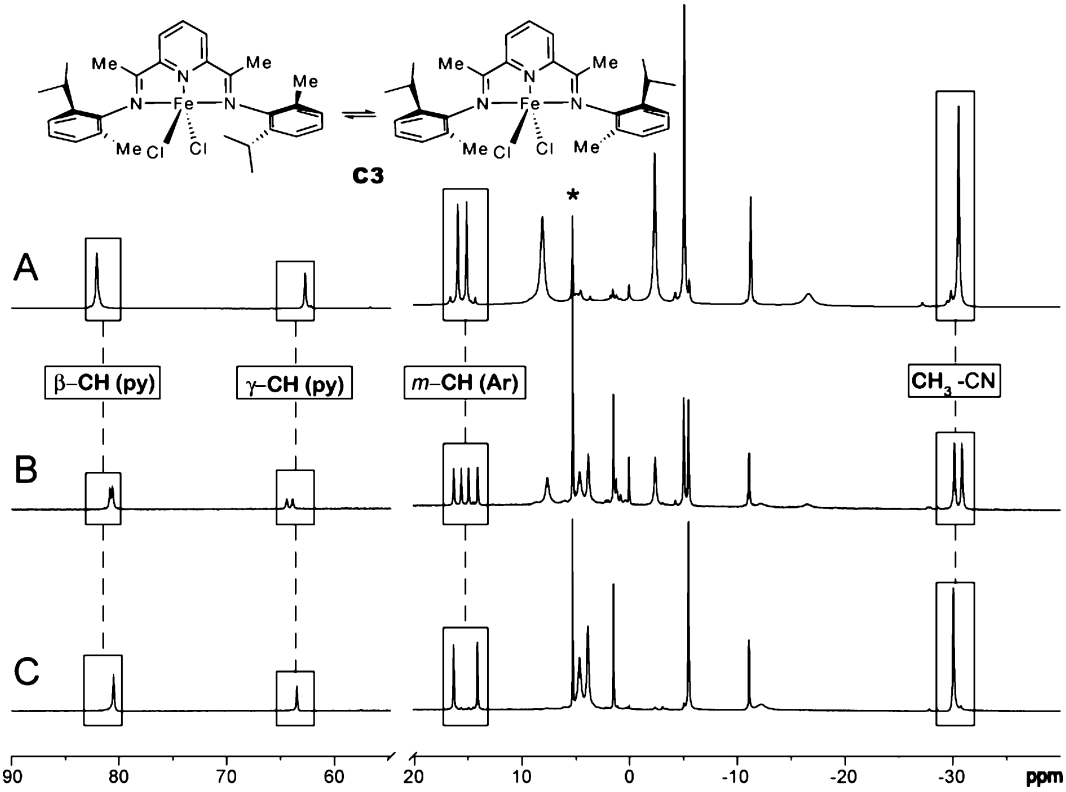

Figure 4. ^{1}H NMR spectra of complex **C3** in CD_2Cl_2 (selected signals assigned; CD_2Cl_2 residual signal marked with an asterisk). (A) Freshly prepared sample directly from the material precipitated during the synthesis (**C3*a***). (B) Spectrum of the same sample, after 24 h at room temperature, showing a 1:1 isomeric mixture. (C) Freshly prepared sample from recrystallized material (**C3*s***).

depending on the solvent used. This procedure can be applied to compounds **C3′** and **C4**, with the same results. The higher solubility of **C6** prevented the carrying out of this procedure in THF, but stirring in hexane/CH_2Cl_2 shifted the **C6*a*/C6*s*** ratio of a solid sample from 1:4 (solution equilibrium value) to 1:10.

The availability of isomerically pure or enriched samples of some FeX_2(PDI) complexes, and their relatively slow interconversion in solution, renders this system suitable for kinetic study. Hence, we monitored the equilibration of the "**a**" isomers in CD_2Cl_2 solution with ^{1}H NMR at different temperatures. In all cases, first-order relaxation kinetics were observed. Figure 5 shows a collective Eyring plot of the direct rate constants, while values for the corresponding activation parameters are collected in Table 1. These are compared to the isomer exchange rate data for ligands **L3** and **L6**. Although the limited range of temperatures accessible for these kinetic studies by NMR (30−40 K) limits the accuracy of their values, they have some useful mechanistic meaning at a qualitative level (as discussed later). At room temperature (298 K), the values of $\Delta G^{\ddagger}$ for the complexes are similar, within a 3 kcal mol^{-1} range, and 1−5 kcal mol^{-1} higher than those found for the free ligands **L3** and **L6** (ca. 20 kcal mol^{-1}).

Note that when using the ***a/s*** terminology we refer only to solubility properties, and so far we have made no assumptions on their actual configurations, since NMR spectra provide no information in this regard. Nevertheless, it seems reasonable to assume that there is a relationship between solubility properties and the structure of the isomers,

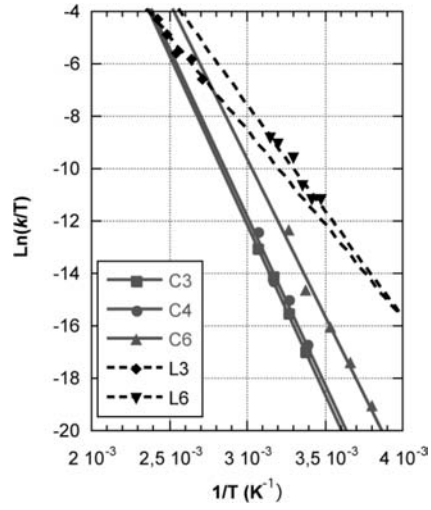

Figure 5. Eyring plot for isomerization processes in solution.

especially for complexes with such similar behavior as **C3**, **C3′**, and **C4**. Supporting this assumption, it is often found that FeX_2(PDI) complexes susceptible to isomerism display the same configuration in their crystal structures if the substitution pattern of the *N*-aryl groups is not very different and the samples were crystallized from similar solvents. Thus, complexes containing 2-Me, 2-CF_3, and 2-Ph groups on the *N*-aryl rings are invariably found in the syn configuration,[3a,b,4f] while others with large aryl groups in the meta position are prone to crystallization as the anti isomers.[3k] Confident that positive structural assignment of the isomeric configurations could be extended at least to the structurally related congeners, we synthesized complex **C9**,

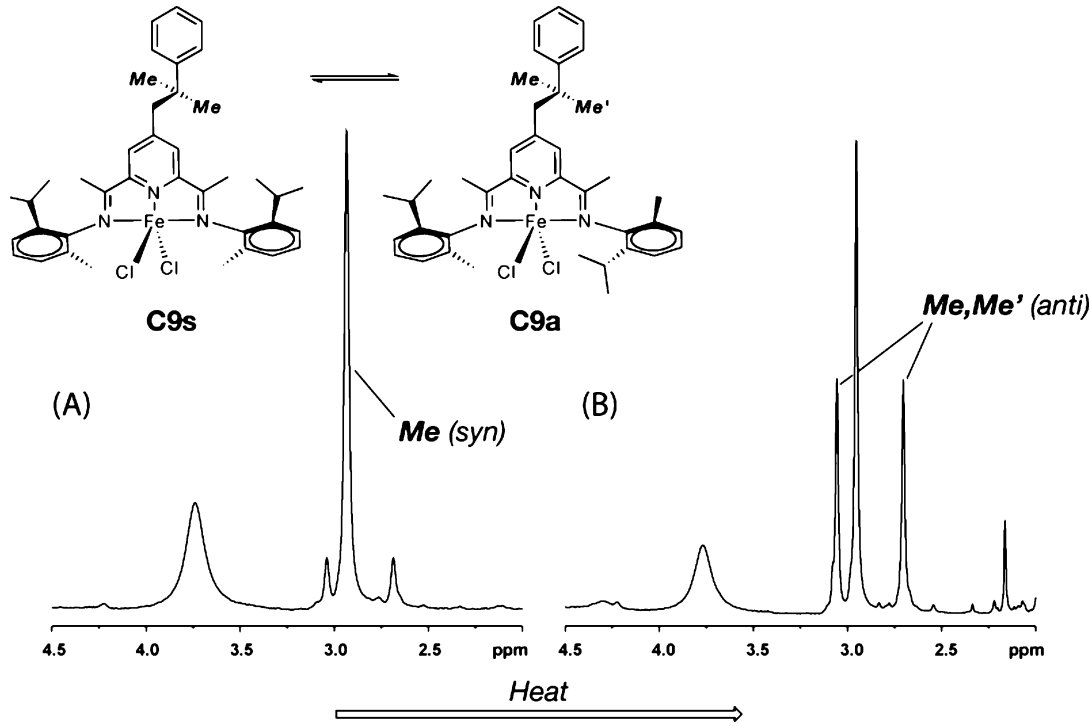

Figure 6. Expansion of the ^{1}H NMR spectrum displaying the neophyl methyl signals (A) of a freshly prepared solution of **C9** in CD_2Cl_2 and (B) the same sample after gentle warming.

an analogue of **C3** displaying a prochiral neophyl group at position 4 of the pyridine ring. We have recently reported that alkyl substitution of this remote position has a negligible influence on the spectroscopic or catalytic properties of FeX_2(PDI) complexes.[7c] Hence, it is not expected to have any effect on the conformational preference of the *N*-aryl groups. The prochiral group reveals the presence or absence of a symmetry mirror in the molecule, as the methyl groups and methylene hydrogen atoms are chemically equivalent in the symmetric syn isomer but become inequivalent in the anti. Since **C9** is quite soluble even in diethyl ether, we found it difficult to prepare isomerically pure samples, but careful recrystallization from CH_2Cl_2/hexane produced essentially one isomer (**C9*s***), and only a small amount (≈10%) of the second isomer (**C9*a***). As expected, the ^{1}H spectrum of **C9** resembles that of **C3**, and this facilitates the identification of several sharp signals (some with almost typically diamagnetic linewidths) corresponding to the remote neophyl group. A narrow signal ($\Delta_{1/2}$ = 8 Hz, relative intensity 6H) at δ 2.98 ppm can be unambiguously assigned to the neophyl CMe_2 group, indicating that **C9s** has the symmetric syn structure. When this sample is warmed at 40 °C for 2 h, the expected isomerization process ensues, until an approximately 1:1 mixture is obtained (Figure 6). These changes are clearly observed in Figure 6, an expansion of the central region of the ^{1}H NMR spectrum of **C9**, before and after isomer equilibration. The splitting of the CMe_2 signal in two at δ 3.04 and 2.69 ppm clearly discloses the asymmetry of the **C9a** diastereoisomer. Comparing the spectra of the **C9** and **C3** (as 1:1 diasteromer mixtures) reveals some common trends, which further support the identification of the isomers. In general, whenever the analogous signals of both spectra are well-resolved **a/s** pairs, the identities of the high- and low-field signals are the same for the **C3** and **C9** mixtures. For example, the two *m*-H's of the **C3a** *N*-aryl groups give rise to two very close signals at δ 15.10 and 15.96 ppm. In the mixture spectrum, the two signals corresponding to **C3s** (δ 16.59, 14.37 ppm) are flanking those of **C3a**, giving rise to a conspicuous feature (see Figure 4). The same is observed in the **C9** system, where the two *m*-H signals of the anti diastereoisomer (δ 16.14, 14.86 ppm) are also flanked by the more separated ones of the syn (δ 16.29, 14.76 ppm). Similar relationships are established for the signals corresponding to the imino methyls, the isopropyl CH and Me groups, and the H3 atoms of the pyridine ring. Such subtle spectral analogies cannot be carried to structurally more distant complexes like **C3′** and **C4**, but it remains reasonable extending the anti, syn configuration assignments to the corresponding **a** and **s** isomers, respectively. The case of complex **C6** is less certain, since this compound displays a slightly different behavior. However, theoretical assessment of the relative energy of the syn and anti configurations suggests that the former relationships hold for **C6** (see below).

Mechanism of the Isomerization Process. Assuming that the source of isomerism is the rotation of the aromatic rings attached to the imine functionality, the energy barrier of the isomer interconversion is caused by the encounter of the α-imino group and the ortho substituents along the least hindered rotation path. Restrictions to rotation essentially disappear in bis(formaldimino)pyridine complexes (α-imine = H), but for complexes with an α-Me group in the imine functionality, the rotation barrier is largely determined by the size of the smaller *N*-aryl ortho substituent. For this reason the energy barrier is very similar in all cases where this substituent is methyl, independently of the size of the

Scheme 2

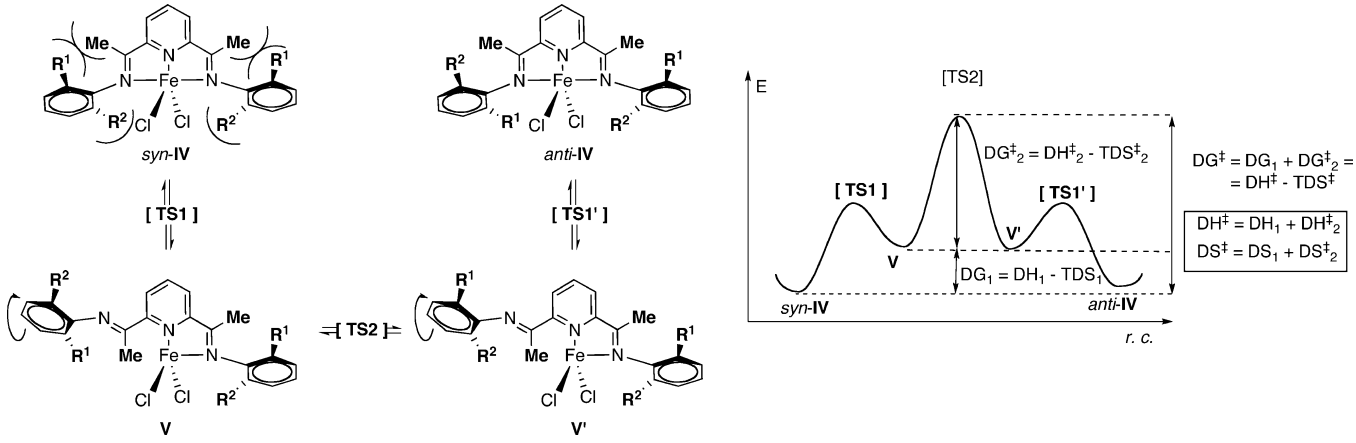

other ortho group. Surprisingly, the energy barrier does not increase appreciably for compound **C4**, which displays *n*-Bu as an α-imino substituent. This indicates that the steric hindrance posed by the primary alkyl in its preferred configuration is almost identical to that caused by a methyl.

The interconversion of syn and anti isomers of the FeX_2(PDI) at room temperature is somewhat surprising when their rigid molecular structure is compared to those of organic compounds that give rise to very stable atropisomers, such as biphenyl derivatives.[19] In spite of the apparently rigid structure of the complexes, data in Table 1 show that coordination of the ligands **L3** or **L6** raises the rotation barrier only 1−5 kcal mol^{-1}. This strongly suggests that aryl group rotation is preceded by the dissociation of the corresponding Fe−N(imine) bond. This dissociative isomerization mechanism is shown in Scheme 2, along with a qualitative energy profile. Assuming that the Fe−N dissociation step is relatively rapid, and the configuration inversion rate is determined by the rotation of the aryl fragment, the overall energy barrier, $\Delta G^{\ddagger}$, can be composed of two terms: the energy required to dissociate the Fe−N bond, ΔG_1, and the activation energy for the rotation step itself, $\Delta G^{\ddagger}_2$. The second term is similar for **C3**, **C6**, and also **C4**, considering the likeliness of their experimental $\Delta G^{\ddagger}$ values.

Since the rotation of the aryl group takes place in the free imine arm of intermediate **V**, the $\Delta G^{\ddagger}_2$ term is expected to be similar to the isomerization energy barrier measured for the free ligands **L3** and **L6**, that is, 20−21 kcal mol^{-1}. Therefore, the Fe−N dissociation energies, ΔG_1, can be estimated as the difference between the rotation barrier of the complexes and that of the free ligands, that is, between 1 and 5 kcal mol^{-1}. The value of ΔG_1 corresponding to the **C6** complex would be the lowest (ca. 1 kcal mol^{-1}). A plausible explanation for this is that the dissociative step is favored by the strain caused by the bulk of the *t*-Bu substituents.

At first glance, the nearly zero activation entropies measured for Fe(PDI) complexes might appear somewhat surprising for a dissociative mechanism. In contrast, activation entropies are negative for the free ligands. Negative $\Delta S^{\ddagger}$ values are often associated with the rotation of rigid molecular fragments,[20] and this has been explained as a result of the restriction of some vibrational modes as the molecule approaches an encumbered transition state.[21] As for the free activation energy, activation entropies of complexes are the sum of the dissociation step thermodynamic entropy (ΔS_1) and the activation parameter linked to the rotation transition step ($\Delta S^{\ddagger}_2$). Assuming that, as found for the free ligands, $\Delta S^{\ddagger}_2$ is negative, it seems plausible that its approximate cancelation by the positive ΔS_1 term leads to near-zero activation entropy values measured for the isomerization of **C3**, **C4**, and **C6**.

Computational Models of the syn−anti Isomerism. With the aim of gaining further understanding of the isomerization mechanism and, at the same time, of providing some additional support to our ideas, we performed DFT calculations on molecular models of the Fe(II)PDI complexes, using the hybrid functional B3LYP. Geometries were optimized using triple-ζ basis functions on the metal center and the atoms directly bound to it (N and halogen), and double-ζ for C and H. Triple-ζ functions were applied to all atoms for energy calculations.

First, we addressed the feasibility of the dissociative step that, according to our proposal, facilitates the rotation process. We decided to investigate the simplified model shown in Figure 7, in order to study the influence of the α-imine substituent (R) and the halogen bound to iron (X).

Calculations show that the dissociation energy of the Fe−N bond of **VI** to afford the tetracoordinated species **VII** is between 0.6 and 6.3 kcal mol^{-1} (Table 2). This is in excellent agreement with the 1−5 kcal mol^{-1} range deduced for the experimental system. When R = H, the dissociated imine group becomes coplanar with the heterocyclic ring, rendering **VII** almost as stable as the pentacoordinated

(19) (a) Carey, A. F.; Sundberg, R. J. *Advanced Organic Chemistry*, 3rd Edition. Part A; Plenum Press: New York, 1990; pp 97−98. (b) Preliminary assessment of the isomerization mechanism using a molecular mechanics model indicated that simple aryl rotation is characterized by high-energy barriers for the acetaldimino derivatives.

(20) Some examples: (a) Lafon, O.; Lesot, P.; Fan, C. A.; Kagan, H. B. *Chem.—Eur. J.* **2006**, *12*, 3772. (b) Pontes, R. M.; Basso, E. A.; dos Santos, F. P. *J. Org. Chem.* **2007**, *72*, 1901. (c) Matchett, S. A.; Zhang, G.; Frattarelli, D. *Organometallics* **2004**, *23*, 5440. (d) Belyakov, P. A.; Shastin, A. V.; Strelenko, Yu. A. *Russ. Chem. Bull., Int. Ed.* **2001**, *50*, 2473. (e) Albéniz, A. C.; Calle, V.; Espinet, P.; Gómez, S. *Inorg. Chem.* **2001**, *40*, 4211.

(21) Li, J. H.; Allinger, N. L. *J. Am. Chem. Soc.* **1989**, *111*, 8566.

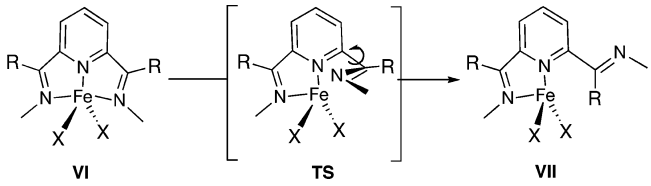

Figure 7. Simplified model used to study the influence of the α-imine substituent (R) and the halogen bound to iron (X).

Table 2. Calculated Energies and Imine−Pyridine Dihedral Angles for the Fe−N Dissociation Step

		dihedral[a] (deg)		energy[b] (kcal mol^{-1})	
R	X	TS	VII	TS	VII
H	Cl	86.3	180.0	10.2	0.6
Me	Cl	92.8	149.9	7.1	4.9
Me	Br	90.1	149.1	8.3	6.3

[a] $N_{py}-C-C=N_{im}$ dihedral angle. [b] Relative to **VI**.

complex **VI**. However, where R = CH_3, the significant steric bulk of the α-Me prevents this from happening, increasing the energy of **VII** relative to **VI**. This increase is not too large but becomes significant for X = Br. It must be noted that the calculation could be somewhat overestimating the Fe−N dissociation energy, since the methyl substitution at nitrogen renders the imine a better ligand than in the real system.

In the calculations, the transition state corresponds to an approximately orthogonal disposition of the free imine arm with regard to the ligand plane. For R = Me, its energy is 7−8 kcal mol^{-1} (Table 2), clearly lower than the experimental $\Delta G^{\ddagger}$ of the real system, which confirms that the dissociative step is rapid in relation to the rotation of the aryl groups. However, for R = H, the Fe−N dissociation barrier is of the same order or slightly higher than that of the facile aryl rotation. This suggests that for formaldimino complexes, isomerization could take place without a dissociative step.

Next, we optimized the structures of three molecular models displaying full substitution paterns in their syn and anti configurations. Models **VIII** and **X** reproduce the structure of complexes **C3** and **C5**, while model **IX** is analogous to **C6** but without the *p*-*t*Bu substituent in the aryl rings. The geometries of the six molecules are shown in Figure 8, and Table 3 lists the computed relative energies for the isomers together with those deduced from solution NMR data. As can be seen in Figure 8, the iron centers tend to display square-pyramidal coordination, which is usually preferred over a trigonal-bipyramidal environment in this kind of complexes. Although the energy differences between the syn and anti configurations are at the limit of the calculation accuracy, the experimental trend is well reproduced by the theoretical calculation. It shows nearly equal stabilities for the isomeric pair **VIII** (describing **C3**), and more significant differences for the isomers **IX** (**C5**) and **X** (like **C6**). In the latter two cases, the energy balance favors the syn configuration, more notably for **X**, where the size difference of the ortho substituents (H and ^{t}Bu) is the largest. In this case, the syn and anti structures have important differences that become noticeable in Figure 8. The syn isomer readily accommodates the iron center in the usually

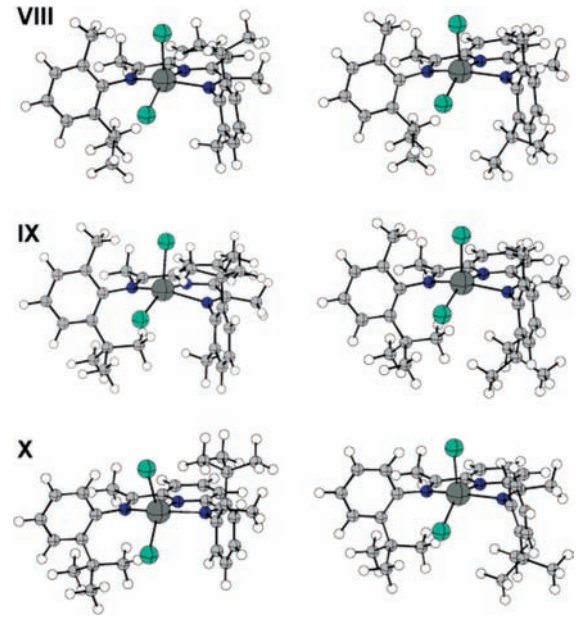

Figure 8. Optimized structures of three molecular models displaying different substituents at the ortho positions of the aryl groups: **VIII**, *i*-Pr and Me; **IX**, *t*-Bu and Me; and **X**, *t*-Bu and H. The syn isomer is shown at the right and the anti at the left.

Table 3. Calculated and Experimental Energy Difference of Calculated Models and Complexes

model molecule	ortho substituents	$\Delta E_{(anti\rightarrow syn)}$ (kcal mol^{-1})[a]	complex	K_{eq}[b]	ΔG_{exp} (kcal mol^{-1})[d]
A	Me, *i*-Pr	+0.33	**C3**	1	0.00
B	Me, *t*-Bu,	−0.61	**C6**	4	−0.82
C	H, *t*-Bu	−2.84	**C5**	10[c]	−1.34

[a] Negative values favor the *syn* isomer. [b] K_{eq} = [major isomer]/[minor isomer], CD_2Cl_2 at RT unless otherwise stated. [c] At 233 K. [d] Calculated from K_{eq}.

preferred square-pyramidal coordination environment, allowing the apical Cl to lie in the least hindered face of the complex. This is not possible in the anti configuration, which bears one bulky ^{t}Bu group on each side ot the molecule, forcing the iron center to become trigonal bipyramidal in order to minimize unfavorable steric interactions with the halide ligands. The same steric effects probably play a similar role in the destabilization of the anti isomer of **IX**. Thus, the calculations suggest that, for **C5** and **C6**, the syn isomer should be preferred in solution. Recalling that, experimentally, **C5*s*** is the most stable isomer in solution, the calculation supports that this has the syn configuration, following the same trend as **C3**, **C3′**, and **C4**.

Conclusions

The ^{1}H NMR spectra of paramagnetic Fe(II)−2,6-bisiminopyridine complexes having *N*-aryl groups with two different substituents at the ortho positions revealed that in solution they exist as geometric isomers, or atropisomers, due to the slow rotation of the aromatic rings. This property is important for their performance as catalysts for α-olefin polymerization or other catalytic processes susceptible to stereochemical control. We synthesized a series of complexes exhibiting different degrees of steric hindrance, and we have shown that the stereochemical stability of such complexes

varies widely. When the ligand substituents are small, isomer interconversion is fast, even on the NMR time scale. However, a moderate degree of steric hindrance suffices to allow the chemical separation of the syn and anti diastereoisomers. We developed a simple procedure based on solubility differences for the preparation of diastereoisomerically pure or enriched samples of these complexes. The actual configuration of these was assigned by the introduction of a prochiral group in the pyridine ring of one of the ligands and was generalized on the basis of the isomer solubility properties.

The availability of these complexes as single diastereoisomers allowed kinetic measurements of the isomerization rates, and the determination of the corresponding activation parameters. Isomerization free activation energies for the complexes are only slightly larger than in the corresponding free ligands, suggesting that the aryl rotation requires the previous dissociation of the Fe−N(imine) bond. This mechanism provides a framework for a consistent interpretation of the isomerization $\Delta H^{\ddagger}$ and $\Delta S^{\ddagger}$ parameters for both complexes and free ligands. This interpretation is further supported by DFT calcultations, whose predictions on the relative stabilities of the isomers and the feasibility of the Fe−N(imine) dissociation closely match the experimental data.

Protocols for the separation of diastereoisomers and the mechanistic insights described in this paper may prove important for the applications of FeX_2(PDI) complexes in stereoselective catalytic processes. We are currently applying these ideas to further improve the stereochemical stability of these complexes.

Experimental Section

Most preparations and other operations were carried out under an oxygen-free nitrogen or argon atmosphere using conventional Schlenk techniques or in a nitrogen-filled glovebox. Conventional organic synthesis procedures were performed under normal air atmosphere. NMR spectra were recorded on a Bruker DRX 300, 400, or 500 MHz spectrometers. ^{1}H and ^{13}C{^{1}H} resonances of the solvents were used as internal standards, but the chemical shifts were reported with respect to TMS. Mycroanalyses were performed by the Mycroanalytical Service of the Instituto de Investigaciones Químicas (Seville, Spain). Infrared and UV−vis spectra were recorded on Bruker Vector 22 and Perkin-Elmer Lambda 12 spectrophotomers, respectively. Magnetic susceptibility measurements were made on a Sherwood Scientific balance, model MSB-Auto. HPLC-grade solvents were freshly distilled prior to use. THF and diethyl ether were distilled under nitrogen from sodium benzophenone; CH_2Cl_2 and chlorobenzene from CaH_2; and hexane, toluene, and benzene from sodium.

Details of the synthesis of ligands, inorganic precursors, and some metal complexes (**C1**, **C2**, **C5**, and **C7**) can be found in the Supporting Information.

Synthesis of the Complexes and Isomer Purification Procedures. Complex C3.[3a] To a stirred suspension of $FeCl_2 \cdot 4H_2O$ (0.795 g, 4.0 mmol) in THF, **L3** (1.0 g, 4.4 mmol, 1.1 equiv) was added at room temperature, and the mixture was stirred for 16 h. The color slowly changed from yellow to deep blue. The suspension was allowed to settle and was filtrated, and the solid was washed with diethyl ether (2 × 20 mL) and hexane (2 × 20 mL). The product was dried under vacuum (1.81 g, 81%). The blue powdery solid was analyzed by ^{1}H NMR, observing a signal pattern that corresponds with that of the isomer **C3a**. Anal. calcd for $C_{29}H_{35}N_3Cl_2Fe$: C, 63.06; H, 6.39; N, 7.61. Found: C, 63.48; H, 7.62; N, 7.45. $\mu_{eff} = 5.7\ \mu_B$ (magnetic balance, 25 °C). ^{1}H NMR of **C3a** (400 MHz, CD_2Cl_2, 298 K): δ 81.29 ($\Delta\nu_{1/2} = 41$ Hz, 2H, *3,5*-CH_{py}), 60.87 ($\Delta\nu_{1/2} = 44$ Hz, 1H, 4-CH_{py}), 15.96 ($\Delta\nu_{1/2} = 19$ Hz, 2H, *m*-C$H_{(ar)}$), 15.10 ($\Delta\nu_{1/2} = 19$ Hz, 2H, *m*-C$H_{(ar)}$), 8.19 ($\Delta\nu_{1/2} = 99$ Hz, 6H, *o*-CH_3), −2.24 ($\Delta\nu_{1/2} = 54$ Hz, 6H, CH(CH_3)$_2$), −4.91 ($\Delta\nu_{1/2} = 18$ Hz, 6H, CH(CH_3)$_2$), −11.03 ($\Delta\nu_{1/2} = 25$ Hz, 2H, *p*-C$H_{(ar)}$), −16.23 ($\Delta\nu_{1/2} = 280$ Hz, 2H, CH(CH$_3$)$_2$), −29.87 ($\Delta\nu_{1/2} = 34$ Hz, 16H, CH_3−C═N). IR (Nujol mull, cm^{-1}): 1625, 1587 (ν(C═N)). UV−vis (CH_2Cl_2): λ_{max} 696 nm ($\varepsilon = 3238$).

Isomerization of C3a. C3a in CD_2Cl_2 was allowed to stand at room temperature under inert atmosphere. After 24 h, a new ^{1}H NMR analysis showed the signals of **C3a** together with a new set of signals corresponding to **C3s** (relative ratio of 1:1). The equilibrium could also be achieved by heating the solution at 40 °C for 3 h. ^{1}H NMR of **C3s** (400 MHz, CD_2Cl_2, 298 K): δ 81.04 ($\Delta\nu_{1/2} = 47$ Hz, 2H, *3,5*-CH_{py}), 60.34 ($\Delta\nu_{1/2c} = 28$ Hz, 1H, *4*-CH_{py}), 16.59 ($\Delta\nu_{1/2} = 20$ Hz, 2H, *m*-C$H_{(ar)}$), 14.37 ($\Delta\nu_{1/2} = 21$ Hz, 2H, *m*-C$H_{(ar)}$), 5.03 ($\Delta\nu_{1/2} = 104$ Hz, 6H, *o*-CH_3), 4.58 ($\Delta\nu_{1/2} = 52$ Hz, 6H, CH(CH_3)$_2$), −5.37 ($\Delta\nu_{1/2} = 18$ Hz, 6H, CH(CH_3)$_2$), −10.96 ($\Delta\nu_{1/2} = 19$ Hz, 2H, *p*-C$H_{(ar)}$), −11.61 ($\Delta\nu_{1/2} = 280$ Hz, 2H, CH(CH$_3$)$_2$), −29.17 ($\Delta\nu_{1/2} = 34$ Hz, 6H, CH_3−C═N).

Rectification of the Isomeric Mixtures of C3. A sample of the mixture **C3a/C3s** (1:1; 0.1 g, 0.18 mmol) was suspended in hexane/dichloromethane (20 mL). The ratio of the solvents (ca. 1:1) was adjusted to allow a slight solubility of the solid (the clear solution has a faint blue color). The suspension was stirred at ambient temperature for 3 days. Upon filtration and drying under a vacuum, the blue isolated solid was identified by ^{1}H NMR as essentially pure **C3s**. In a similar experiment, the isomeric mixture (0.1 g, 0.18 mmol) was suspended in THF and stirred at room temperature for 3 days. Upon filtration and drying under a vacuum, the blue isolated solid was identified by ^{1}H NMR as essentially pure **C3a**.

Complex C3′. $FeBr_2$ (0.43 g, 2.0 mmol) was suspended in THF (15 mL), and a solution of **L3′** (0.89 g, 2.1 mmol) in THF (15 mL) was added dropwise at room temperature. The color of the resultant yellow mixture slowly changed to deep-blue. The suspension was stirred for 24 h and was allowed to settle. The liquid phase was removed by filtration, and the blue solid was washed with diethylether (20 mL) and hexane (20 mL). The blue residue was dried under a vacuum (0.91 g, 71%). The ^{1}H NMR spectra of the solid show signals which correspond to the mixture of isomers in a relative ratio of 9:1, for the major product, **C3′a**, relative to the minor, **C3′s**. Anal. calcd for $C_{29}H_{35}N_3Br_2Fe$: C, 54.32; H, 5.50; N, 6.55. Found: C, 53.95; H, 5.27; N, 6.60. $\mu_{eff} = 5.5\ \mu_B$ (magnetic balance, 25 °C). IR (Nujol mull, cm^{-1}): 1613, 1584 (ν(C═N)). UV−vis (CH_2Cl_2): λ_{max} 686 nm ($\varepsilon = 2643$). Equilibration and rectification procedures analogous to those described for **C3** allowed the preparation of pure samples of the two isomers. ^{1}H NMR of **C3′a** (400 MHz, CD_2Cl_2, 298 K): δ 76.09 ($\Delta\nu_{1/2} = 51$ Hz, 2H, *3,5*-CH_{py}), 71.06 ($\Delta\nu_{1/2} = 29$ Hz, 1H, *4*-CH_{py}), 15.91 ($\Delta\nu_{1/2} = 20$ Hz, 2H, *m*-C$H_{(ar)}$), 15.16 ($\Delta\nu_{1/2} = 18$ Hz, 2H, *m*-C$H_{(ar)}$), 8.94 ($\Delta\nu_{1/2} = 107$ Hz, 6H, *o*-CH_3), 2.02 ($\Delta\nu_{1/2} = 50$ Hz, 6H, CH(CH_3)$_2$), −4.09 ($\Delta\nu_{1/2} = 19$ Hz, 6H, CH(CH_3)$_2$), −11.52 ($\Delta\nu_{1/2} = 17$ Hz, 2H, *p*-C$H_{(ar)}$), −26.13 ($\Delta\nu_{1/2} = 29$ Hz, 6H, CH_3−C═N). ^{1}H NMR of **C3′s** (400 MHz, CD_2Cl_2, 298 K): δ 75.87 ($\Delta\nu_{1/2} = 39$ Hz, 2H, *3,5*-CH_{py}), 72.48 ($\Delta\nu_{1/2} = 28$ Hz, 1H, *4*-CH_{py}), 15.81 ($\Delta\nu_{1/2} = 20$ Hz, 2H, *m*-C$H_{(ar)}$), 15.49 ($\Delta\nu_{1/2} = 18$ Hz, 2H, *m*-C$H_{(ar)}$), 10.60 ($\Delta\nu_{1/2} =$

117 Hz, 6H, *o*-CH_3), −0.03 ($\Delta\nu_{1/2}$ = 47 Hz, 6H, CH(CH_3)$_2$), −4.17 ($\Delta\nu_{1/2}$ = 22 Hz, 6H, CH(CH_3)$_2$), −11.52 ($\Delta\nu_{1/2}$ = 17 Hz, 2H, *p*-C$H_{(ar)}$), −26.65 ($\Delta\nu_{1/2}$ = 34 Hz, 6H, CH_3−C═N).

Complex C4. A solution of $FeCl_2 \cdot 4H_2O$ (0.30 g, 1.5 mmol) in THF (15 mL) was treated with **L4** (0.82 g, 1.6 mmol) in THF, added dropwise at room temperature. The color and nature of the mixture changed as described before. The reaction mixture was stirred for 24 h and the solvent removed by filtration. The solid was washed with diethyl ether (10 mL) and hexane (10 mL). The resultant product was dried under a vacuum (0.736 g, 77%). The ^{1}H NMR spectrum showed signals of essentially pure **C4a**. Anal. calcd for $C_{35}H_{47}N_3Cl_2Fe$: C, 66.04; H, 7.44; N, 6.60. Found: C, 66.40; H, 7.35; N, 6.42. μ_{eff} = 5.48 μ_B (magnetic balance, 25 °C). IR (Nujol mull, cm^{-1}): 1575 (ν(C═N)). UV−vis (CH_2 Cl_2): λ_{max} 697 nm (ε = 2400). Equilibration and rectification procedures analogous to those described for **C3** allowed the prepation of pure samples of the two isomers. ^{1}H NMR of **C4a** (300 MHz, CD_2Cl_2, 298 K): δ 83.27 ($\Delta\nu_{1/2}$ = 55 Hz, 2H, *3,5*-CH_{py}), 77.16 ($\Delta\nu_{1/2}$ = 27 Hz, 1H, *4*-CH_{py}), 16.24, ($\Delta\nu_{1/2}$ = 27 Hz, 2H, *m*-C$H_{(ar)}$), 14.21 ($\Delta\nu_{1/2}$ = 23 Hz, 2H, *m*-C$H_{(ar)}$), 4.77 ($\Delta\nu_{1/2}$ = 128 Hz, 6H, *o*-CH_3), −1.46 ($\Delta\nu_{1/2}$ = 18 Hz, 6H, CH_3−C), −3.79 ($\Delta\nu_{1/2}$ = 23 Hz, 6H, CH(CH_3)$_2$), −11.96 ($\Delta\nu_{1/2}$ = 37 Hz, 2H, *p*-C$H_{(ar)}$), −13.77 ($\Delta\nu_{1/2}$ = 69 Hz, 6H, CH(CH_3)$_2$), −15.30 ($\Delta\nu_{1/2}$ = 275 Hz, 2H, CH(CH_3)$_2$). ^{1}H NMR of **C4s** (300 MHz, CD_2Cl_2, 298 K): δ 82.94 ($\Delta\nu_{1/2}$ = 50 Hz, 2H, *3,5*-CH_{py}), 79.46 ($\Delta\nu_{1/2}$ = 27 Hz, 1H, 4-CH_{py}), 16.36 ($\Delta\nu_{1/2}$ = 23 Hz, 2H, *m*-C$H_{(ar)}$), 14.21 ($\Delta\nu_{1/2}$ = 23 Hz, 2H, *m*-C$H_{(ar)}$), −1.19 ($\Delta\nu_{1/2}$ = 23 Hz, 6H, CH_3−C), −4.30 ($\Delta\nu_{1/2}$ = 18 Hz, 6H, CH(CH_3)$_2$).

Complex C6. A solution of **L6** (0.39 g, 0.7 mmol) in diethylether (10 mL) was added to a stirred suspension of $FeCl_2$(dme) (140 mg, 0.64 mmol) in the same solvent (10 mL). The color of the suspension changed to blue. The mixture was kept under vigorously stirring for 40 min. A blue solid precipitated and was isolated by filtration, washed with cold (0 °C) diethylether (3 × 20 mL), and dried under a vacuum (0.23 g, 47%). ^{1}H NMR showed essentially pure **C6a**, although signals corresponding to ca. 10% of isomer **C6s** were also detected. μ_{eff} = 5.33 μ_B (magnetic balance, 25 °C). UV−vis (CH_2 Cl_2): λ_{max}, 674 nm (ε = 1298). IR (Nujol mull, cm^{-1}): 1605, 1579 (ν(C═N)). Equilibration in CD_2Cl_2 at room temperature leads to a 1:4 mixture of **C6a** and **C6s**, and this proportion changed to 10:1 by stirring in hexane with a small amount of dichloromethane. ^{1}H NMR of **C6a** (400 MHz, CD_2Cl_2, 298 K): δ 88.42 ($\Delta\nu_{1/2}$ = 120 Hz, 2H, *3,5*-CH_{py}), 45.62 ($\Delta\nu_{1/2}$ = 127 Hz, 1H, *4*-CH_{py}), 13.54 ($\Delta\nu_{1/2}$ = 20 Hz, 2H, *m*-C$H_{(ar)}$), 12.55 ($\Delta\nu_{1/2}$ = 20 Hz, 2H, *m*-C$H_{(ar)}$), 3.86 ($\Delta\nu_{1/2}$ = 85 Hz, 6H, *o*-CH_3), 2.35 ($\Delta\nu_{1/2}$ = 7 Hz, 18H, *o*-^{t}Bu), −13.04 ($\Delta\nu_{1/2}$ = 115 Hz, 18H, *p*-^{t}Bu), −15.54 ($\Delta\nu_{1/2}$ = 18 Hz, 6H, CH_3−C═N). ^{1}H NMR of **C6s** (400 MHz, CD_2Cl_2, 298 K): δ 83.61($\Delta\nu_{1/2}$ = 139 Hz, 2H, *3,5*-CH_{py}), 52.22 ($\Delta\nu_{1/2}$ = 364 Hz, 1H, *p*-CH_{py}), 16.42 ($\Delta\nu_{1/2}$ = 19 Hz, 2H, *m*-C$H_{(ar)}$), 8.75 ($\Delta\nu_{1/2}$ = 19 Hz, 2H, *4*-C$H_{(ar)}$), 1.64 ($\Delta\nu_{1/2}$ = 10 Hz, 18H, *o*-^{t}Bu), −5.96 ($\Delta\nu_{1/2}$ = 202 Hz, 6H, *o*-CH_3), −7.67 ($\Delta\nu_{1/2}$ = 190 Hz, 18H, *p*-^{t}Bu), −17.07 ($\Delta\nu_{1/2}$ = 52 Hz, 6H, CH_3−C═N).

Complex C8. The monoimine complex {$FeCl_2$[2-(CH_3CO)-6-(CH_3C(N-Mes)C_5H_3N]-*κ*-*O*,*N*,*N*} (see the Supporting Information; 20.8 g, 51 mmol) was suspended in chlorobenzene (150 mL), and 2-isopropylaniline (14.9 mL, 102 mmol) was added. The reaction mixture was stirred for 6 days at 55 °C. The suspension was filtered, and the resultant blue solid was washed with diethylether (2 × 50 mL) and hexane (1 × 50 mL) and dried under vacuum for 3 days (26.04 g, 97%). The excess of aniline could be easily recovered by evaporation of the filtrate to dryness. Anal. calcd for $C_{27}H_{31}N_3Cl_2Fe$: C, 61.85; H, 5.96; N, 8.01. Found: C, 61.85; H, 5.81; N, 7.71. μ_{eff} = 4.97 μ_B (magnetic balance, 25 °C). ^{1}H NMR (400 MHz, CD_2Cl_2, 298 K): δ 81.29, ($\Delta\nu_{1/2}$ = 85 Hz, 1H, *3- or 5*-CH_{py}), 80.12 ($\Delta\nu_{1/2}$ = 85 Hz, 1H, *3 or 5*-CH_{py}), 30.75 ($\Delta\nu_{1/2}$ = 91 Hz, 1H, *4*-CH_{py}), 24.11 ($\Delta\nu_{1/2}$ = 207 Hz, 3H, *o*-CH_3), 21.61 ($\Delta\nu_{1/2}$ = 54 Hz, 3H, *p*-CH_3), 19.43 ($\Delta\nu_{1/2}$ = 140 Hz, 1H, *m*-C$H_{(ar2)}$), 15.98 ($\Delta\nu_{1/2}$ = 99 Hz, 1H, *m*-C$H_{(ar1)}$), 12.33 ($\Delta\nu_{1/2}$ = 55 Hz, 1H, *m*-C$H_{(ar1)}$), 11.85 ($\Delta\nu_{1/2}$ = 146 Hz, 1H, *m*-C$H_{(ar2)}$), 6.22 ($\Delta\nu_{1/2}$ = 244 Hz, 6H, CH(CH_3)$_2$), 5.03 ($\Delta\nu_{1/2}$ = 244 Hz, 3H, *o*-CH_3), −4.35 ($\Delta\nu_{1/2}$ = 140 Hz, 6H, CH(CH_3)$_2$), −12.50 ($\Delta\nu_{1/2}$ = 54 Hz, 2H, *p*-C$H_{(ar2)}$), −12.50 ($\Delta\nu_{1/2}$ = 54 Hz, 6H, CH_3−C═N), −19.54 ($\Delta\nu_{1/2}$ = 158 Hz, 1H, *o*-C$H_{(ar2)}$), −25.30 ($\Delta\nu_{1/2}$ = 73 Hz, 6H, CH_3−C═N). IR (Nujol mull, cm^{-1}): 1621, 1587 (ν(C═N)). UV−vis (CH_2Cl_2): λ_{max} 708 nm (ε = 1872).

Complex C9. $FeCl_2$(dme) (0.96 g, 0.57 mmol) in diethylether (20 mL) was treated with **L9** (0.38 g, 0.63 mmol) and stirred at room temperature for 16 h. The color of the mixture changed to blue, but no precipitate was observed. The solution was evaporated to dryness and the residue extracted with CH_2Cl_2 (10 mL); traces of unreacted $FeCl_2$(dme) were separated by filtration. The solution was taken to dryness and the residue dried, washed with diethyl ether (2 × 20 mL) and hexane (2 × 20 mL), and dried under a vacuum (191 mg, 50%). The solid was analyzed by ^{1}H NMR; two set of signals were observed, which corresponded to the isomeric mixture anti/syn **C9** in a relative ratio of 1:1. Careful recrystallization of the mixture with CH_2Cl_2/hexane (1:1) at −20 °C for 15 days afforded a blue microcrystaline solid, which was identified by ^{1}H NMR as the *syn*-**C9** (**C9s**) isomer. Anal. calcd for $C_{39}H_{47}Cl_2FeN_3 \cdot 1/3CH_2Cl_2$: C, 66.27; H, 6.74; N, 5.89. Found: C, 66.31; H, 6.99; N, 5.85. ^{1}H NMR of **C9s** (400 MHz, CD_2Cl_2, 298 K): δ 82.91($\Delta\nu_{1/2}$ = 53 Hz, 2H, *3,5*-CH_{py}), 16.29, 14.76 ($\Delta\nu_{1/2}$ = 19 Hz, 4H, *m*-C$H_{(ar)}$), 8.77 ($\Delta\nu_{1/2}$ = 15 Hz, 2H, *m*-C$H_{(Neo)}$), 7.41 ($\Delta\nu_{1/2}$ = 18 Hz, 2H, *o*-C$H_{(Neo)}$), 7.05 ($\Delta\nu_{1/2}$ = 17 Hz, 2H, *p*-C$H_{(Neo)}$), 6.21 ($\Delta\nu_{1/2}$ = 93 Hz, 6H, *o*-CH_3), 3.74 ($\Delta\nu_{1/2}$ = 46 Hz, 6H, CH(CH_3)$_2$), 2.98 ($\Delta\nu_{1/2}$ = 8 Hz, 6H, C(*Me*)$_2$), −3.77 ($\Delta\nu_{1/2}$ = 19 Hz, 6H, CH(CH_3)$_2$), −4.10 ($\Delta\nu_{1/2}$ = 23 Hz, 2H, CH_2), −8.26 ($\Delta\nu_{1/2}$ = 267 Hz, 2H, CH(CH_3)$_2$), −9.43 ($\Delta\nu_{1/2}$ = 20 Hz, 2H, *p*-C$H_{(ar)}$), −17.48 ($\Delta\nu_{1/2}$ = 45 Hz, 6H, CH_3−C═N). IR (Nujol mull, cm^{-1}): 1589 (ν(C═N)). UV−vis (CH_2 Cl_2): λ_{max} 685 nm (ε = 1421). ^{1}H NMR of **C9a** (400 MHz, CD_2Cl_2, 298 K): δ 83.18 ($\Delta\nu_{1/2}$ = 53 Hz, 2H, *m*-CH_{py}), 16.14, 14.86 ($\Delta\nu_{1/2}$ = 19 Hz, 4H, *m*-C$H_{(ar)}$), 9.60 ($\Delta\nu_{1/2}$ = 93 Hz, 6H, *o*-CH_3), 8.71 ($\Delta\nu_{1/2}$ = 15 Hz, 2H, *m*-C$H_{(Neo)}$), 7.37 ($\Delta\nu_{1/2}$ = 18 Hz, 2H, *o*-C$H_{(Neo)}$), 7.05 ($\Delta\nu_{1/2}$ = 17 Hz, 2H, *p*-C$H_{(Neo)}$), 3.04 and 2.69 ($\Delta\nu_{1/2}$ = 8 Hz, 6H, C(*Me*)$_2$), −1.66 ($\Delta\nu_{1/2}$ = 46 Hz, 6H, CH(CH_3)$_2$), −3.77 ($\Delta\nu_{1/2}$ = 19 Hz, 6H, CH(CH_3)$_2$), −4.10 ($\Delta\nu_{1/2}$ = 23 Hz, 2H, CH_2), −9.43 ($\Delta\nu_{1/2}$ = 20 Hz, 2H, *p*-C$H_{(ar)}$), −14.10 ($\Delta\nu_{1/2}$ = 267 Hz, 2H, CH(CH_3)$_2$), −18.01 ($\Delta\nu_{1/2}$ = 45 Hz, 6H, CH_3−C═N).

Kinetic Studies. These were done by NMR. Samples were prepared in the glovebox by dissolving a known amount (4−6 mg) of the corresponding complex (**C3a**, **C3a′**, **C4a**, or **C6**) or ligand (**L6**) in CD_2Cl_2 (0.6 mL) and immediately placing the sample in the spectrometer probe, which was previously stabilized at the desired temperature. The sample was allowed to stabilize for 4−5 min. ^{1}H NMR spectra were recorded periodically until no further change was observed. Progress of the equilibration process was monitored by integration of a well-resolved pair of signals, one for each isomer. Probe temperatures were measured with a standard $CH_3OH/CDCl_3$ calibration sample.

Computational Details. Electronic structures and geometries of the model complexes were computed within the density functional theory at the B3LYP level,[22] using the 6-311G* basis set for Fe, Cl, and N and 6-31G* for C and H atoms of the PDI

(22) (a) Becke, A. D. *J. Chem. Phys.* **1993**, *98*, 5648. (b) Lee, C.; Wang, Y.; Parr, R. G. *Phys. Rev. B* **1988**, *37*, 785.

ligands. Me, *i*-Pr, and *t*-Bu substituents on phenyl rings have been described using the 3-21G* basis set. A single-point energy calculation was performed on all optimized structures using the 6-311+G(2d,p) basis set. Vibrational frequency calculations were done by diagonalization of the analytically computed Hessian to ensure that the optimized structures were real minima (Nimag = 0) or maxima (Nimag = 1). All calculations were performed using the Gaussian 03 package.[23] Figures were drawn using Molekel.[24] XYZ coordinates of all optimized complexes are available upon request.

Acknowledgment. Financial support from the DGI (Project CTQ2006-05527/BQU), Junta de Andalucía (Project P06-FQM-01704), and Repsol-YPF is gratefully acknowledged. A.M.N. and M.A.C. are thankful for predoctoral grants from CSIC (I3P and JAE programs), and C.M.P. is thankful for a research contract from Repsol-YPF. A.R.-D. and D.R. acknowdlege postdoctoral contracts from the Ministerio de Educación y Ciencia (Ramón y Cajal program) and the European Union (sixth Framework Program Marie Curie Outgoing International Fellowship), respectively. We thank Dr. I. Urban (IIQ) for helpful discussions.

Supporting Information Available: Details of the synthesis of ligands, inorganic precursors, and some metal complexes (**C1**, **C2**, **C5**, and **C7**). This material is available free of charge via the Internet at http://pubs.acs.org.

IC802271Y

(23) Frisch, M. J.; Trucks, G. W.; Schlegel, H. B.; Scuseria, G. E.; Robb, M. A.; Cheeseman, J. R.; Montgomery, J. A., Jr.; Vreven, T.; Kudin, K. N.; Burant, J. C.; Millam, J. M.; Iyengar, S. S.; Tomasi, J.; Barone, V.; Mennucci, B.; Cossi, M.; Scalmani, G.; Rega, N.; Petersson, G. A.; Nakatsuji, H.; Hada, M.; Ehara, M.; Toyota, K.; Fukuda, R.; Hasegawa, J.; Ishida, M.; Nakajima, T.; Honda, Y.; Kitao, O.; Nakai, H.; Klene, M.; Li, X.; Knox, J. E.; Hratchian, H. P.; Cross, J. B.; Adamo, C.; Jaramillo, J.; Gomperts, R.; Stratmann, R. E.; Yazyev, O.; Austin, A. J.; Cammi, R.; Pomelli, C.; Ochterski, J. W.; Ayala, P. Y.; Morokuma, K.; Voth, G. A.; Salvador, P.; Dannenberg, J. J.; Zakrzewski, V. G.; Dapprich, S.; Daniels, A. D.; Strain, M. C.; Farkas, O.; Malick, D. K.; Rabuck, A. D.; Raghavachari, K.; Foresman, J. B.; Ortiz, J. V.; Cui, Q.; Baboul, A. G.; Clifford, S.; Cioslowski, J.; Stefanov, B. B.; Liu, G.; Liashenko, A.; Piskorz, P.; Komaromi, I.; Martin, R. L.; Fox, D. J.; Keith, T.; Al-Laham, M. A.; Peng, C. Y.; Nanayakkara, A.; Challacombe, M.; Gill, P. M. W.; Johnson, B.; Chen, W.; Wong, M. W.; Gonzalez, C.; Pople, J. A. *Gaussian 03*, revision C.02; Gaussian, Inc.: Wallingford, CT, 2004.

(24) Portmann, S.; Luthi, H. P. *Chimia* **2000**, *54*, 766.